



HAL
open science

Environmental and social inequities in continental France: an analysis of exposure to heat, air pollution, and lack of vegetation

Lucie Adélaïde, Ian Hough, Emie Seyve, Itai Kloog, Grégory Fifre, Guy Launoy, Ludivine Launay, Mathilde Pascal, Johanna Lepeule

► **To cite this version:**

Lucie Adélaïde, Ian Hough, Emie Seyve, Itai Kloog, Grégory Fifre, et al.. Environmental and social inequities in continental France: an analysis of exposure to heat, air pollution, and lack of vegetation. *Journal of Exposure Science and Environmental Epidemiology*, 2024, 10.1038/s41370-024-00641-6 . hal-04444139

HAL Id: hal-04444139

<https://hal.science/hal-04444139>

Submitted on 7 Feb 2024

HAL is a multi-disciplinary open access archive for the deposit and dissemination of scientific research documents, whether they are published or not. The documents may come from teaching and research institutions in France or abroad, or from public or private research centers.

L'archive ouverte pluridisciplinaire **HAL**, est destinée au dépôt et à la diffusion de documents scientifiques de niveau recherche, publiés ou non, émanant des établissements d'enseignement et de recherche français ou étrangers, des laboratoires publics ou privés.

1 **Environmental and social inequities in continental France: An analysis of exposure to heat, air**
2 **pollution, and lack of vegetation**

3 Lucie Adélaïde^{a,b}, Ian Hough^{b,c}, Emie Seyve^{b,d}, Itai Kloog^{c,e}, Grégory Fifre^f, Guy Launoy^{g,h}, Ludivine
4 Launay^{g,i,j}, Mathilde Pascal^{*a}, Johanna Lepeule^{*b}

5 * These authors contributed equally to this work.

6 ^aSanté publique France, 12 rue du Val d’Osne, 94415 Saint-Maurice Cedex, France

7 ^bUniversité Grenoble Alpes, Inserm, CNRS, IAB, Site Santé, Allée des Alpes, 38700 La Tronche,
8 France

9 ^cDepartment of Geography and Environmental Development, Ben-Gurion University of the Negev,
10 Be’er Sheva, Israel

11 ^dUniversité de Paris Cité, Inserm, INRAE, Centre of Research in Epidemiology and StatisticS (CRESS),
12 75000 Paris, France

13 ^eDepartment of Environmental Medicine and Public Health, Icahn School of Medicine at Mount Sinai,
14 New York, NY, USA

15 ^fMétéo-France, 73 avenue de Paris, 94165 Saint-Mandé Cedex, France

16 ^gU1086 Inserm Anticipa, Avenue Général Harris, 14076 Caen Cedex, France

17 ^hUniversity Hospital of Caen, 14076 Caen Cedex, France

18 ⁱPlateforme MapInMed, US PLATON, Avenue Général Harris, 14076 Caen Cedex, France

19 ^jCentre François Baclesse, Avenue Général Harris, 14076 Caen Cedex, France

20

21 **Corresponding author:**

22 Lucie Adélaïde, lucie.adelaide@santepubliquefrance.fr, Santé publique France, 12 rue du Val d’Osne,
23 94415 Saint-Maurice Cedex, France

24 Johanna Lepeule, johanna.lepeule@univ-grenoble-alpes.fr, Université Grenoble Alpes, Inserm, CNRS,
25 IAB, Site Santé, Allée des Alpes, 38700 La Tronche, France

26

27 *This preprint has not undergone peer review or any post-submission improvements or corrections. The*
28 *Version of Record of this article is published in Journal of Exposure Science & Environmental*
29 *Epidemiology, and is available online at <https://doi.org/10.1038/s41370-024-00641-6>.*

30 **ABSTRACT**

31 **BACKGROUND**

32 Cumulative environmental exposures and social deprivation increase health vulnerability and limit the
33 capacity of populations to adapt to climate change.

34 **OBJECTIVE**

35 Our study aimed at providing a fine-scale characterization of exposure to heat, air pollution, and lack of
36 vegetation in continental France between 2000 and 2018, describing spatiotemporal trends and
37 environmental hotspots (i.e., areas that cumulate the highest levels of overexposure), and exploring any
38 associations with social deprivation.

39 **METHODS**

40 The European (EDI) and French (FDep) social deprivation indices, the normalized difference vegetation
41 index, daily ambient temperatures, particulate matter (PM_{2.5} and PM₁₀), nitrogen dioxide, and ozone
42 (O₃) concentrations were estimated for 48,185 French census districts. Reference values were chosen to
43 characterize (over-)exposure. Hotspots were defined as the areas cumulating the highest overexposure
44 to temperature, air pollution, and lack of vegetation. Associations between heat overexposure or hotspots
45 and social deprivation were assessed using logistic regressions.

46 **RESULTS**

47 Overexposure to heat was higher in 2015-2018 compared with 2000-2014. Exposure to all air pollutants
48 except for O₃ decreased during the study period. In 2018, more than 79% of the urban census districts
49 exceeded the 2021 WHO air quality guidelines. The evolution of vegetation density between 2000 and
50 2018 was heterogeneous across continental France. In urban areas, the most deprived census districts
51 were at a higher risk of being hotspots (odds ratio (OR): 10.86, 95% CI: 9.87-11.98 using EDI and OR:
52 1.07, 95% CI: 1.04-1.11 using FDep).

53 **SIGNIFICANCE**

54 This nationwide fine-scale study provides a framework to identify environmental hotspots and reveals
55 social inequalities in the cumulative exposure to heat, air pollutants, and lack of vegetation, in France.
56 This approach lends support to the inclusion of environmental and social inequities in adaptation
57 strategies to climate change.

58 **KEYWORDS:** temperature, particulate matter, green spaces, social deprivation, hotspots,
59 environmental justice

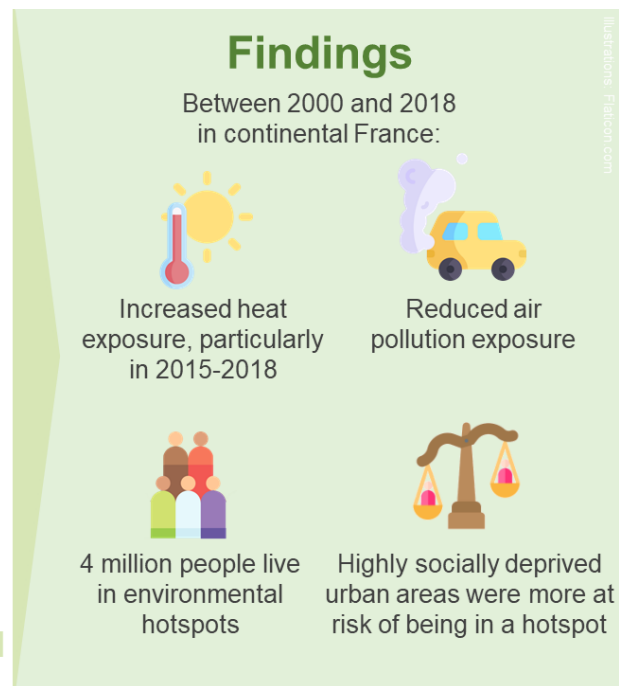
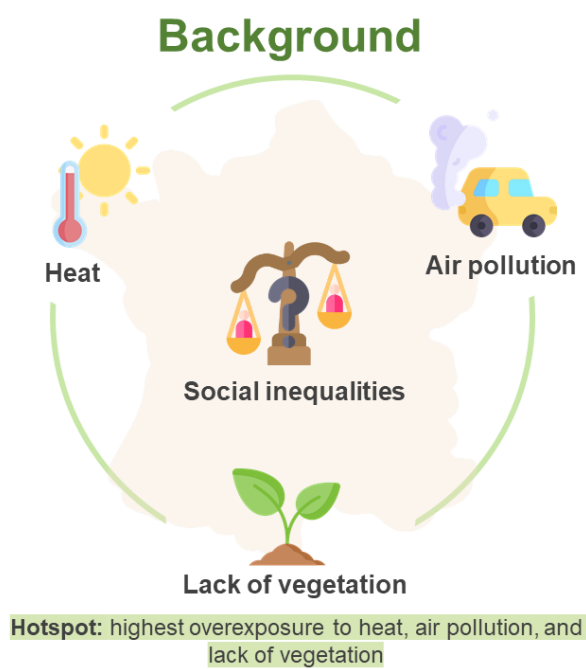
60

61 **IMPACT STATEMENT**

62 We studied cumulative environmental exposures and social deprivation in French census districts. The
63 2015-2018 period showed the highest overexposure to heat between 2000 and 2018. In 2018, the air
64 quality did not meet the 2021 WHO guidelines in most census districts and 8.6 million people lived in
65 environmental hotspots. Highly socially deprived urban areas had a higher risk of being in a hotspot.
66 This study proposes for the first time, a methodology to identify hotspots of exposure to heat, air
67 pollution, and lack of vegetation and their associations with social deprivation at a national level.

68

69 **GRAPHICAL ABSTRACT**



70

71 INTRODUCTION

72 In the context of rapid climate change, heat exposure associated with the cumulative exposure to
73 multiple environmental factors and social deprivation can increase health vulnerabilities and limit the
74 capacity of exposed populations to adapt to climate change. This not only raises serious public health
75 concerns but is also a source of injustice, as unequal exposure to environmental risks and unequal access
76 to environmental goods such as parks and forests result in environmental inequities.

77 In Europe, areas with cumulative exposure to multiple environmental stressors tend to be more deprived
78 (1, 2). Depending on their location, the deprived or poorer areas may be more exposed to heat (3), have
79 lower green space availability (4, 5), and/or be more exposed air pollution (4, 6, 7).

80 Exposure to heat and air pollution has multiple synergistic health effects such as cardiovascular or
81 respiratory morbidity and negative reproductive outcomes (8-11). Vegetation plays a protective role
82 against heat (12, 13) and air pollution (14) and has numerous health benefits on mental health, cognitive
83 function, cardiovascular morbidity, and pregnancy outcomes among others (15). In addition,
84 socioeconomic characteristics influence the population's ability to avoid or adapt to these environmental
85 health hazards (2).

86 In accordance with a holistic planetary health approach, reducing cumulative exposure to environmental
87 risks and social deprivation should be at the heart of both public health policies and climate policies. A
88 preliminary step in this direction is to produce comprehensive data to describe, analyze, and compare
89 environmental exposures in time and space. However, to our knowledge, no study to date has
90 investigated cumulative exposure to heat, air pollution, lack of vegetation, and social deprivation at a
91 fine geographical scale and at the national level. Describing cumulative exposure at a national level
92 allows the characterization of poorly studied territories and the targeting of heat adaptation interventions
93 to the areas and populations most at risk.

94 Existing studies mostly focus on air pollution and, to a lesser extent, on vegetation, and are limited to
95 city-level or regional analyses (16). However, air pollution, vegetation, and heat are interdependent.
96 Vegetation contributes to air and surface cooling and thermal comfort through solar radiation absorption,
97 evapotranspiration, evaporation, albedo modification, and radiative shading (17). It also reduces ambient
98 air pollution by increasing the deposition of particulate matter (PM) and absorbing gaseous pollutants
99 (14, 18) as well as by promoting non-motorized transport (18). Vegetation can also act as a physical
100 barrier against pollutants, thus reducing their dispersion. However, this barrier effect may
101 simultaneously increase pollutant concentrations on roads and reduce exposure to air pollution on the
102 other side of this barrier (18). Vegetation also emits biogenic volatile organic compounds (bVOC),
103 which can react with other chemical species that form secondary particles. For example, isoprene
104 emissions associated with NO_x contribute to ozone (O₃) formation. Monoterpenes and sesquiterpenes
105 can increase PM_{2.5} and PM₁₀ concentrations (14). Heat increases air pollution through ozone formation

106 due to UV radiation in the presence of nitrogen dioxide (NO₂) (19). Air pollutants such as O₃ have a
107 negative effect on vegetation growth by affecting the metabolic function of leaves (20). More broadly,
108 the presence of vegetation and favorable meteorological conditions have a positive impact on human
109 behavior and thus indirectly influence air pollution. Describing cumulative exposure to heat, air
110 pollution, and lack of vegetation could thus help support adaptation policies.

111 Our study aimed to characterize fine-scale exposure to heat, air pollution, and lack of vegetation across
112 continental France between 2000 and 2018, to describe spatiotemporal trends and environmental
113 hotspots (i.e., areas that cumulate the highest levels of overexposure), and to explore any associations
114 with social deprivation.

115

116 **MATERIALS AND METHODS**

117 **Study area and period**

118 Drawing on the 2021 geography reference files, we analyzed the 48,185 IRIS of the 34,477
119 municipalities located in the 94 departments of continental France for the period 2000-2018. An IRIS is
120 a sub-municipal geographical unit equivalent to a census district (21). Large municipalities (> 5,000
121 inhabitants) are divided into several IRIS, while smaller municipalities constitute their own IRIS. IRIS
122 is the smallest geographical unit for which French census data are available.

123 **Data**

124 *Urbanization*

125 The 2021 urbanization level of each municipality and IRIS were obtained from the National Institute of
126 Statistics and Economic Studies (INSEE). INSEE distinguishes between urban and rural municipalities
127 depending on their population density. Densely populated municipalities and municipalities of
128 intermediate density were defined as urban municipalities. Low-density and sparsely populated
129 municipalities were considered rural municipalities (22).

130 *Population*

131 Population data (i.e., number of inhabitants) were obtained from INSEE at the IRIS level for the period
132 2014-2018 and at the municipality level for 2006-2018 (23). The population at the IRIS level for 2006-
133 2013 was estimated using the evolution percentage of the population at the municipality level. The
134 evolution percentage E for the year i and municipality j was thus:

$$135 \quad E_{i,j} = \frac{\text{population}_{i,j}}{\text{population}_{i+1,j}}$$

136 Where *population* was the number of inhabitants. Then, the estimated population *populationest* for
137 each IRIS *k* was calculated as follows:

$$138 \quad \text{populationest}_{i,j,k} = \text{population}_{i+1,j} \times E_{i,j}$$

139 Due to the lack of harmonized data prior to 2006, we assumed that the population of each IRIS was
140 constant between 2000 and 2006.

141 *Climate types*

142 We used the classification of the French meteorological information system, Météo-France, which
143 categorizes French municipalities into eight different climates (Supplementary Figure 1): mountain
144 climate, semi-continental climate and climate of mountainous margins, modified oceanic climate,
145 transitional oceanic climate, oceanic climate, moderate Mediterranean climate, southwest basin climate,
146 and Mediterranean climate (24).

147 *Temperature*

148 Daily minimum, mean, and maximum temperatures from 2000 to 2018 were obtained from a multi-
149 resolution model with a 200 m² resolution for large urban areas (> 50,000 inhabitants) and 1 km² across
150 the rest of continental France (25). These estimates were generated using spatiotemporal models based
151 on Météo-France weather station data, satellite land surface temperature data, and additional spatial and
152 temporal predictors such as the normalized difference vegetation index (NDVI), elevation, and land
153 cover. Hough et al. provides more in-depth modeling methodologies and performance results (25). Daily
154 exposure to minimum, mean, and maximum temperatures for each IRIS was estimated by calculating
155 the area-weighted average gridded temperature data.

156 *Vegetation*

157 To approximate the level of vegetation, we used the NDVI, a greenness indicator ranging from -1 to +1,
158 with higher values indicating denser vegetation. The NDVI was derived from Landsat satellite images
159 with a 30 m spatial resolution (26). Mean summer (i.e., from June 1 to August 31 each year) NDVI was
160 computed for each year between 2000 and 2018.

161 For each IRIS, the annual mean summer NDVI was estimated by calculating the area-weighted average
162 of the gridded NDVI data.

163 *Air pollution concentrations*

164 Daily mean PM_{2.5} and PM₁₀ concentrations from 2000 to 2018 were obtained at a 1 km² resolution across
165 continental France from a multi-stage ensemble model combining air quality monitoring data, satellite-
166 derived aerosol optical depth, and other spatiotemporal predictors such as meteorological parameters,
167 NDVI, and elevation (27). The increases observed in 2008-2009 for PM_{2.5} and in 2007 for PM₁₀ were

168 due to a change in the measurement techniques used by the national air quality monitoring stations to
169 include semi-volatile PM (27, 28). We used daily mean NO₂ and daily maximum O₃ concentrations
170 estimated by the French Institute for Industrial Environment and Risks (INERIS) based on models
171 combining background measurements of air quality monitoring stations and modeling of the chemistry
172 transport model with a spatial resolution of around 4 km for the period 2000-2017 and around 2 km for
173 2018 (29).

174 For each IRIS, daily exposure to PM_{2.5}, PM₁₀, NO₂, and O₃ was estimated by calculating the area-
175 weighted average of the gridded concentration data.

176 *Social deprivation*

177 We used the 2015 version of two deprivation indices: the European Deprivation Index (EDI) (30) and
178 the French Deprivation Index (FDep) (31) at the IRIS level. Both indices are composite measures based
179 on a combination of census data to characterize the socioeconomic environment of the IRIS.

180 The EDI is a European index constructed using Eurostat data and capable of measuring relative
181 deprivation in a transcultural way across all European countries. Its French version is a weighted
182 combination of ten census variables grouped into two dimensions: a material dimension (non-
183 homeowners, households without a car, households with more than two occupants, overcrowded
184 dwellings with more than one person per room) and a social dimension (unemployment, foreigners,
185 unskilled workers, low education level, single-parent households, unmarried status) (32). The FDep is
186 computed using principal component analysis from four census variables: median household income,
187 proportion of secondary school graduates (15 years and over), proportion of laborers in the active
188 population, and proportion of unemployment in the active population.

189 The first quintile of FDep and EDI represents the least deprived IRIS, while the fifth quintile the most
190 deprived.

191 We considered both indicators, because a clear concordance between them has not yet been
192 demonstrated (33, 34), and there is currently no recommendation favoring one of them (32).

193 **Reference values to describe relative exposure to environmental factors**

194 Relative exposure to heat, air pollution, and lack of vegetation was assessed by defining the reference
195 values to harmonize the description of exposures, thus facilitating the interpretation of temperature and
196 NDVI exposure across climate types. These indicators are summarized in Supplementary Table 1.

197 *Heat*

198 A climatological approach based on 10-day means was used to develop a reference for each IRIS. 10-
199 day temperature means smoothed the data while accounting for climatic variability over time. The

200 reference 10-day mean, minimum, and maximum temperatures d_m were computed over the period
201 2000-2018 for each department and each type of climate as follows:

$$202 \quad d_m = \frac{\sum_{n=2000}^{2018} \frac{\sum_{l=1}^{10} T_{l,m,n}}{10}}{19}$$

203 Where T was the daily temperature (i.e., Tmean, Tmin, or Tmax) for the l^{th} day (from 1 to 365), period
204 of 10 days m (from 1 to 37), and year n (from 2000 to 2018). Then, the daily difference between daily
205 temperatures and the corresponding 10-day reference values $\Delta T_{l,m,n}$ (i.e., relative temperature indicators
206 ΔT_{mean} , ΔT_{min} , or ΔT_{max}) for each IRIS was thus:

$$207 \quad \Delta T_{l,m,n} = T_{l,m,n} - d_m$$

208 This approach allowed us to identify the IRIS overexposed to heat compared to other IRIS with similar
209 geographical and climatological conditions. This also provides a proxy to identify the urban heat island.

210 ΔT_{mean} , ΔT_{min} , and ΔT_{max} were averaged by season: in this dataset, summer from June 21 to
211 September 22, autumn from September 23 to December 21, winter from December 22 to March 19, and
212 spring from March 20 to June 20.

213 *Lack of vegetation*

214 For each type of climate, reference values were defined as the median values of the mean summer NDVI
215 in rural areas, as rural areas were assumed to be closer to the most vegetated areas than urban areas.
216 Lack of vegetation was then assessed each year for each IRIS by calculating the difference between the
217 mean summer NDVI and the reference value (ΔNDVI).

218 *Air pollution*

219 To identify the IRIS overexposed to air pollution, the WHO air quality guidelines developed to protect
220 public health were used as reference values (35).

221 The annual and summer mean differences between daily mean $\text{PM}_{2.5}$, PM_{10} , and NO_2 concentrations and
222 annual WHO air quality guideline values ($5 \mu\text{g}/\text{m}^3$, $15 \mu\text{g}/\text{m}^3$, and $10 \mu\text{g}/\text{m}^3$, respectively) were
223 calculated ($\Delta \text{PM}_{2.5}$, ΔPM_{10} , ΔNO_2) for each IRIS. For O_3 , the summer mean difference between daily
224 maximum concentrations and WHO air quality guideline values for the peak season ($60 \mu\text{g}/\text{m}^3$) was
225 calculated (ΔO_3) for each IRIS.

226 **Cumulative exposure indicator and identification of environmental hotspots**

227 A cumulative exposure indicator with four classes was created for each IRIS and each year
228 (Supplementary Table 1) based on the distribution quartiles of the environmental factors according to
229 the period (2000-2004, 2005-2009, 2010-2014, 2015-2018) and urbanization level (urban/rural).

230 Hotspots (class 4) were defined as IRIS with the highest overexposure to all factors: (i) summer ΔT_{mean}
231 in the last quartile, (ii) at least one of the four air pollution indicators (annual $\Delta \text{PM}_{2.5}$, annual ΔPM_{10} ,
232 annual ΔNO_2 , or summer ΔO_3) in the last quartile, and (iii) summer ΔNDVI in the first quartile. IRIS of
233 class 1 had the lowest exposure quartiles for all factors. IRIS of class 2 and class 3 were in the upper
234 quartiles for one and two factors, respectively.

235 **Statistical analysis**

236 *Descriptive analysis and temporal evolution of indicators*

237 The number and percentage of IRIS by deprivation index quintiles were described according to
238 urbanization level. The evolution of summer ΔT_{mean} , summer ΔT_{min} , summer ΔT_{max} , summer
239 ΔNDVI , annual ΔNO_2 , summer ΔO_3 , annual $\Delta \text{PM}_{2.5}$, and annual ΔPM_{10} concentrations was described
240 between 2000 and 2018. Analyses were stratified by urbanization level (urban/rural) and by 4- to 5-year
241 periods (2000-2004, 2005-2009, 2010-2014, 2015-2018). Heat indicators (ΔT_{mean} , ΔT_{min} , ΔT_{max})
242 were described by season and climate type.

243 Spearman correlation coefficients for the exposure indicators (summer ΔT_{mean} , summer ΔT_{min} ,
244 summer ΔT_{max} , annual and summer $\Delta \text{PM}_{2.5}$, annual and summer ΔPM_{10} , annual and summer ΔNO_2 ,
245 summer ΔO_3 , and summer ΔNDVI) and between EDI and FDep were computed for the entire period
246 2000-2018 and by urbanization level.

247 Exposure indicators (summer ΔT_{mean} , summer ΔNDVI , annual $\Delta \text{PM}_{2.5}$, annual ΔPM_{10} , annual ΔNO_2 ,
248 and summer ΔO_3) were described according to the deprivation index quintiles and the cumulative
249 exposure indicator class, with a focus on hotspots.

250 *Associations between environmental exposure and social deprivation*

251 Associations between environmental exposure indicators and social deprivation were studied by (i)
252 regressing hotspots (yes/no) (main analysis) and then (ii) regressing the cumulative exposure indicator
253 (four classes) against each social deprivation index (EDI and FDep) by quintiles using (i) binary logistic
254 regressions and (ii) non-ordinal polytomous logistic regressions.

255 Given that heat exposure arouses special interest in climate adaptation policies and that its reduction can
256 only be achieved through indirect actions such as planting vegetation or reducing air pollution, we used
257 non-ordinal polytomous logistic regressions to investigate the association between the categorized
258 summer ΔT_{mean} and the categorized indicators summer ΔNDVI , $\Delta \text{PM}_{2.5}$, ΔNO_2 , and ΔO_3 adjusted for
259 deprivation indices (EDI and FDep) and year (Supplementary Table 1). We included an interaction term
260 between social deprivation indices and environmental exposure indicators.

261 All analyses were stratified by urbanization level.

262

263 **RESULTS**

264 **Descriptive analysis and temporal evolution of indicators**

265 Overall, 64% of the 48,185 IRIS were classified as rural, and the main climate type was the modified
 266 oceanic climate (Supplementary Figure 1). Highly socially deprived IRIS (quintile 5) were more likely
 267 to be in urban areas than in rural areas, especially using the EDI (40.3% of urban IRIS vs. 7.5% of rural
 268 IRIS) (Table 1).

269 **Table 1.** Distribution of IRIS by quintiles and urbanization level

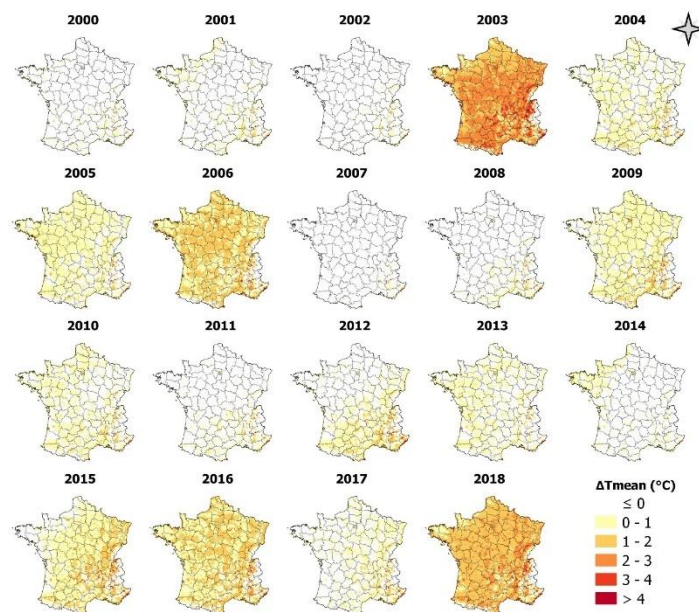
	EDI		FDep	
	Urban IRIS n (%)	Rural IRIS n (%)	Urban n (%)	Rural IRIS n (%)
Quintile 1	2,118 (12.1 %)	7,346 (24.0 %)	5,882 (33.5 %)	3,743 (12.2 %)
Quintile 2	2,011 (11.5 %)	7,436 (24.3 %)	3,069 (17.5 %)	6,503 (21.2 %)
Quintile 3	2,223 (12.7 %)	7,169 (23.3 %)	2,383 (13.6 %)	7,203 (23.5 %)
Quintile 4	2,988 (17.0 %)	6,383 (20.8 %)	2,102 (12.0 %)	7,500 (24.5 %)
Quintile 5	7,067 (40.3 %)	2,296 (7.5 %)	3,954 (23.0 %)	5,687 (18.6 %)
Missing	1,135 (6.5 %)	13 (<0.01 %)	152 (0.01%)	7 (<0.01 %)
Total	17,542	30,643	17,542	30,643

270
 271 Concerning the exposure indicators, the summers of 2003, 2006, 2016, and 2018 had the highest mean
 272 ΔT_{mean} in both urban and rural areas and across all climate types (Figures 1A and 2; Supplementary
 273 Figure 2). More generally, for all seasons and across all periods, mean ΔT_{mean} , ΔT_{min} , and ΔT_{max}
 274 were higher in urban IRIS than in rural IRIS (Supplementary Table 2). The 2015-2018 period showed
 275 the highest summer ΔT_{mean} , ΔT_{min} , and ΔT_{max} for both urban and rural areas.



276 **Figure 1.** Evolution of (A) mean summer ΔT_{mean} and ΔNDVI , (B) mean annual ΔNO_2 and ΔO_3
 277 evolution and (C) mean annual $\Delta \text{PM}_{2.5}$ and ΔPM_{10} between 2000 and 2018 in urban and rural IRIS in
 278 continental France. // corresponds to the inclusion of semi-volatile particulate matter.

279



280

281

Figure 2. Mean summer ΔT_{mean} between 2000 and 2018 in continental France

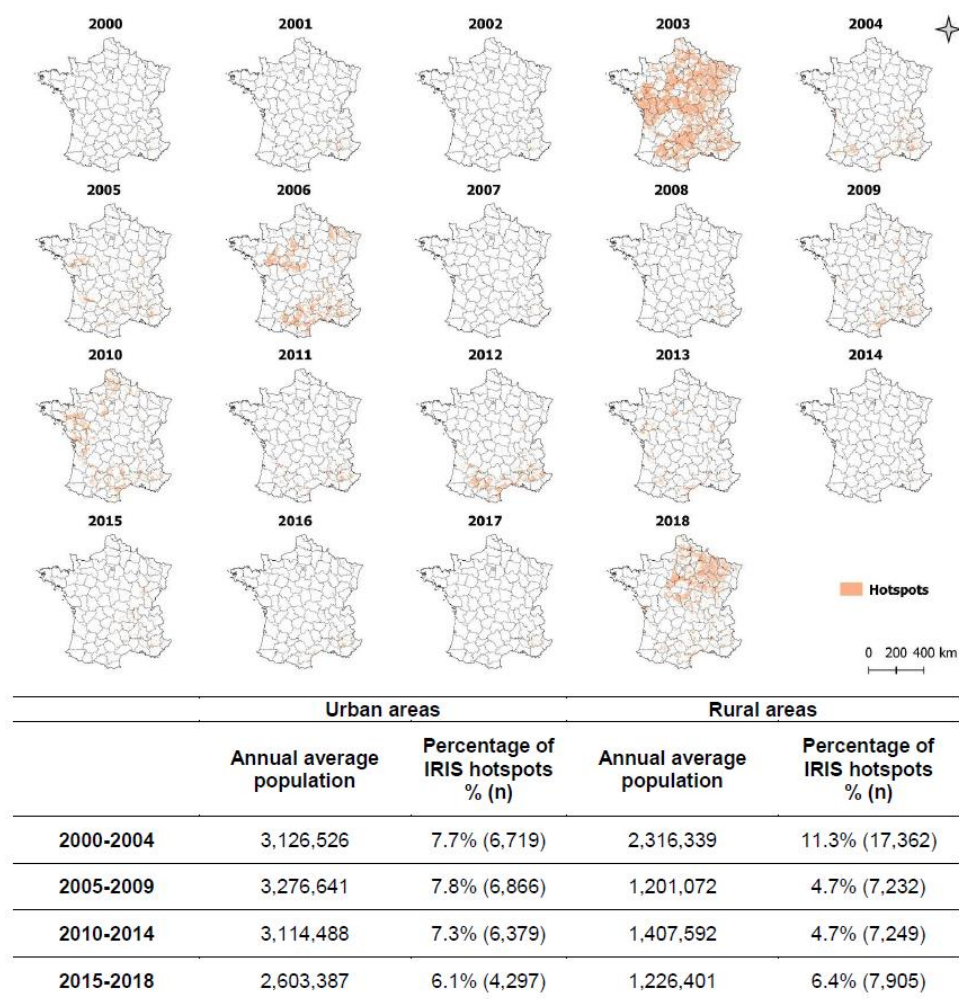
282 Summer mean ΔNDVI was characterized by a decrease in 2003 and a marked spatial heterogeneity
 283 between 2000 and 2018 (Figure 1A; Supplementary Figure 3). During this period, ΔNO_2 dropped by
 284 55.9% in urban IRIS (from $18.5 \mu\text{g}/\text{m}^3$ in 2000 to $8.1 \mu\text{g}/\text{m}^3$ in 2018) and by 89.8% in rural IRIS (from
 285 $8.4 \mu\text{g}/\text{m}^3$ in 2000 to $0.86 \mu\text{g}/\text{m}^3$ in 2018) (Figure 1B). For ΔO_3 , two sharp increases were observed in
 286 2003 and 2018 (Figure 1B). In 2018, almost all IRIS (93.7%) in urban areas exceeded the WHO air
 287 quality guideline levels ($> 10 \mu\text{g}/\text{m}^3$) for NO_2 compared with 59.3% in rural areas. For O_3 , all IRIS were
 288 above these guidelines in 2018 ($> 60 \mu\text{g}/\text{m}^3$). On average, ΔNO_2 and ΔO_3 were higher in urban areas
 289 than in rural areas (Supplementary Figure 4).

290 Since 2009, $\Delta \text{PM}_{2.5}$ and ΔPM_{10} have steadily decreased in urban and rural areas (Figure 1C). Mean
 291 $\Delta \text{PM}_{2.5}$ dropped by 54.6% (from $13.0 \mu\text{g}/\text{m}^3$ in 2009 to $5.9 \mu\text{g}/\text{m}^3$ in 2018) in urban IRIS and by 67.9%
 292 (from $9.4 \mu\text{g}/\text{m}^3$ in 2009 to $3.0 \mu\text{g}/\text{m}^3$ in 2018) in rural IRIS. Despite these reductions, 99.9% and 78.7%
 293 of urban IRIS and 97.6% and 20.0% of rural IRIS exceeded the WHO air quality guidelines for $\text{PM}_{2.5}$
 294 and PM_{10} , respectively, in 2018 ($> 5 \mu\text{g}/\text{m}^3$ and $> 15 \mu\text{g}/\text{m}^3$). On average, $\Delta \text{PM}_{2.5}$ and ΔPM_{10}
 295 concentrations were higher in urban areas than in rural areas (Supplementary Figure 5).

296 In both urban and rural areas, the different summer ΔT indicators were positively correlated with
 297 summer ΔO_3 and negatively (or close to 0) correlated with ΔPM and ΔNO_2 (Supplementary Figure 6).
 298 Summer ΔNDVI was negatively correlated with all pollutant and temperature indicators. In urban IRIS,
 299 EDI and FDep showed different correlation patterns with the environmental exposure indicators.
 300 According to EDI, the most deprived IRIS in urban areas were more exposed to heat (summer ΔT_{mean}),
 301 air pollution (annual $\Delta \text{PM}_{2.5}$, ΔPM_{10} , and ΔNO_2), and lack of vegetation (summer ΔNDVI). For
 302 example, mean ΔT_{mean} and annual $\Delta \text{PM}_{2.5}$ were respectively $+0.68 \text{ }^\circ\text{C}$ and $+9.6 \mu\text{g}/\text{m}^3$ in highly

303 socially deprived IRIS (quintile 5) versus +0.35 °C and +8.35 µg/m³ in the least deprived IRIS (quintile
 304 1). Summer ΔO₃ remained stable across EDI quintiles. This pattern was not observed in rural areas.
 305 With FDep, a U-shaped relationship was observed in urban areas in which the least and most deprived
 306 IRIS were more exposed to air pollution (annual ΔPM_{2.5}, ΔPM₁₀, and ΔNO₂) and lack of vegetation
 307 (summer ΔNDVI). In rural areas, a higher FDep was associated with a lower exposure to all air
 308 pollutants (Supplementary Figures 7 and 8).

309 In terms of cumulative exposure, most IRIS (70.0%) were class 2 (i.e., in the strongest quartiles for one
 310 factor) (Supplementary Table 3). On average, 6.8% of rural IRIS were classified as hotspots (i.e., IRIS
 311 in the strongest quartiles for all factors) (1,554,243 inhabitants) versus 7.2% of urban IRIS
 312 (3,052,728 inhabitants) (Figure 3). While the percentage of hotspots was rather stable in urban areas
 313 (6.0% to 8.0%), it was the highest in 2000-2004 (11.3%) in rural areas (mainly due to 2003, which
 314 recorded the highest number of hotspots for the entire period 2000-2018) and then increased again in
 315 2015-2018 (6.5%) compared with 2005-2014 (4.7%).

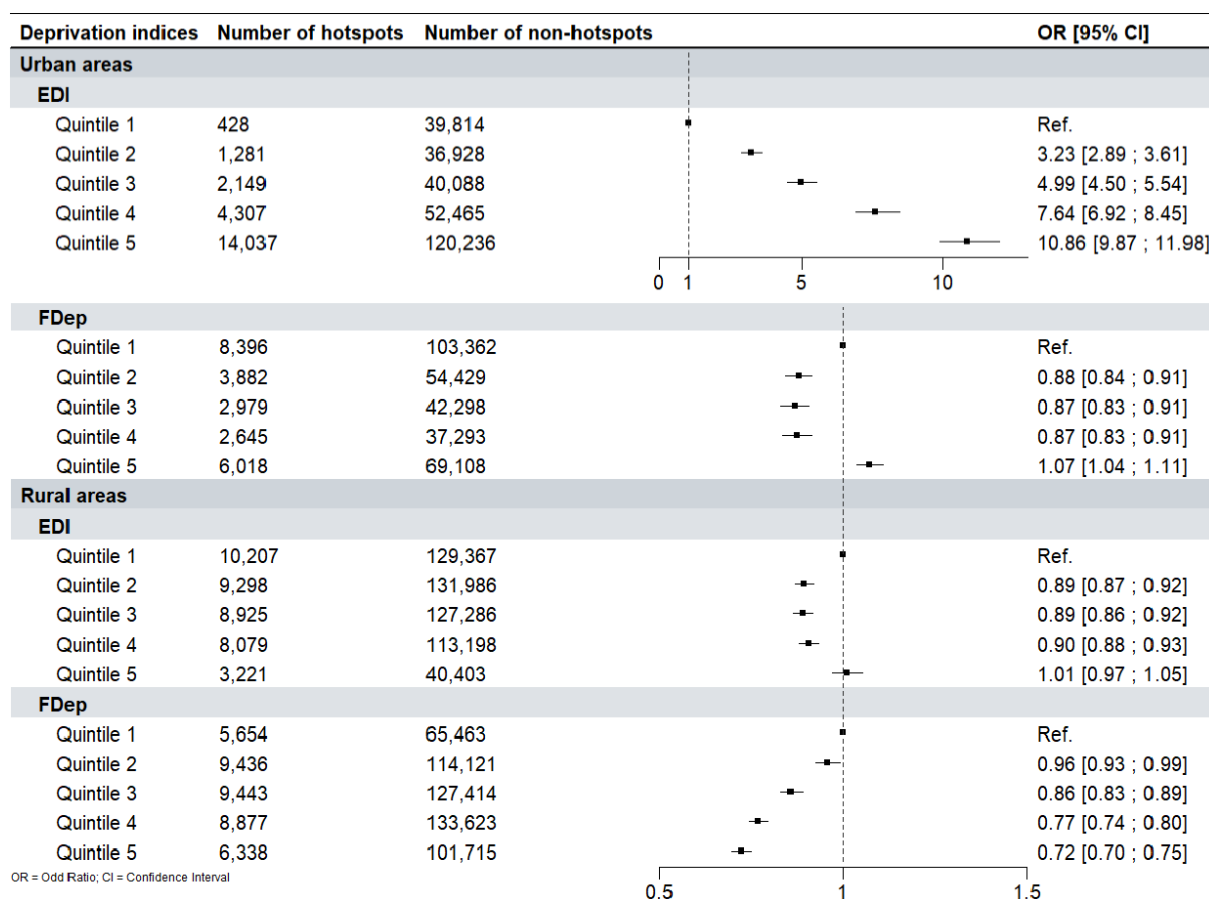


316 **Figure 3.** Spatial distribution of IRIS hotspots by year, annual average population living in an IRIS
 317 hotspot, and percentage of IRIS hotspots by period and urbanization level between 2000 and 2018 in
 318 continental France

319 Exposures were higher in urban hotspots than in rural hotspots (Supplementary Figure 9). For example,
 320 IRIS hotspots were exposed to mean summer ΔT_{mean} of $+1.9\text{ }^{\circ}\text{C}$ in urban areas and $+1.7\text{ }^{\circ}\text{C}$ in rural
 321 areas compared with non-hotspots. For annual $\Delta \text{PM}_{2.5}$, summer ΔO_3 , and summer ΔNDVI in urban and
 322 rural hotspots, these differences were respectively $+2.7\text{ }\mu\text{g}/\text{m}^3$ versus $+0.92\text{ }\mu\text{g}/\text{m}^3$, $+15.60\text{ }\mu\text{g}/\text{m}^3$ versus
 323 $+17.91\text{ }\mu\text{g}/\text{m}^3$, and -0.20 versus -0.15 . The mean percentages of IRIS overexposed to each environmental
 324 exposure indicator according to the cumulative exposure indicator class and urbanization level are
 325 presented in Supplementary Table 4.

326 Associations between environmental exposure and social deprivation

327 In urban areas, increased deprivation was strongly associated with the risk of being in a hotspot
 328 ($p < 0.001$) based on EDI (Figure 4). With FDep, this association was only observed for highly socially
 329 deprived IRIS (quintile 5) ($p < 0.001$) with a U-shaped relationship between social deprivation and the
 330 risk of living in a hotspot. In rural areas, higher social deprivation was negatively associated with the
 331 risk of being in a hotspot for both EDI and FDep.



332 **Figure 4.** Associations between hotspots and non-hotspots and deprivation indices (EDI and FDep)
 333 between 2000 and 2018 in urban and rural areas in continental France. OR (95% CI) estimated by
 334 binary logistic regressions.
 335

336 Using EDI and in urban areas, the risk of cumulating several exposures increased with social
 337 deprivation, regardless of the cumulative exposure class (Supplementary Figure 10). In rural areas, a U-
 338 shaped relationship was observed. Using FDep, a U-shaped relationship was observed in urban areas,
 339 whereas a decreasing risk with social deprivation was found in rural areas.

340 In summer, IRIS were more likely to have a medium or high exposure to heat if they also had a medium
 341 or high exposure to a lack of vegetation or to O₃ in both urban and rural areas (models 1 and 2, Table 2).
 342 In rural areas, they were more likely to have a medium or high exposure to heat if they also had a medium
 343 or high exposure to PM_{2.5} (models 1 and 2). In urban areas, IRIS were less likely to have a medium or
 344 high exposure to heat if they had a high exposure to NO₂ or medium exposure to PM_{2.5}. In both urban
 345 and rural areas, highly socially deprived IRIS (quintile 5) were at a lower risk of being exposed to high
 346 heat.

347 **Table 2.** Associations between (over-)exposure to heat (ΔT_{mean}) and deprivation indices (EDI and
 348 FDep), lack of vegetation, and air pollutants during summer between 2000 and 2018 in urban and rural
 349 areas of continental France (OR [95% CI]^a)

	Urban areas		Rural areas	
	Medium overexposure to heat	High overexposure to heat	Medium exposure to heat	High exposure to heat
Model 1				
EDI				
Quintile 1	Ref.	Ref.	Ref.	Ref.
Quintile 2	1.82 [1.43; 2.31]	2.77 [1.91; 4.01]	1.53 [1.28; 1.82]	2.66 [2.05; 3.46]
Quintile 3	1.33 [1.05; 1.70]	0.67 [0.46; 0.98]	1.70 [1.43; 2.02]	1.16 [0.89; 1.50]
Quintile 4	0.90 [0.71; 1.14]	0.27 [0.19; 0.40]	0.68 [0.56; 0.83]	0.27 [0.20; 0.36]
Quintile 5	1.88 [1.51; 2.33]	0.91 [0.64; 1.29]	1.04 [0.71; 1.52]	0.31 [0.18; 0.52]
ΔNDVI exposure (lack of vegetation)				
Low	Ref.	Ref.	Ref.	Ref.
Medium	2.31 [2.17; 2.46]	3.69 [3.39; 4.02]	1.21 [1.16; 1.26]	1.53 [1.44; 1.62]
High	10.8 [9.63; 12.0]	52.8 [46.2; 60.4]	1.15 [1.11; 1.20]	1.58 [1.49; 1.68]
ΔPM_{2.5} exposure				
Low	Ref.	Ref.	Ref.	Ref.
Medium	0.62 [0.55; 0.70]	0.49 [0.42; 0.57]	3.35 [3.07; 3.65]	10.0 [8.86; 11.4]
High	0.61 [0.53; 0.70]	0.51 [0.43; 0.60]	6.38 [5.81; 7.01]	18.7 [16.3; 21.6]
ΔNO₂ exposure				
Low	Ref.	Ref.	Ref.	Ref.

Medium	0.69 [0.63; 0.76]	0.45 [0.40; 0.51]	0.84 [0.80; 0.89]	0.75 [0.70; 0.80]
High	0.53 [0.47; 0.59]	0.27 [0.24; 0.32]	0.71 [0.68; 0.74]	0.81 [0.75; 0.87]
ΔO_3 exposure				
Low	Ref.	Ref.	Ref.	Ref.
Medium	2.79 [2.37; 3.29]	10.4 [7.83; 13.9]	2.89 [2.57; 3.26]	9.02 [7.57; 10.7]
High	6.06 [5.12; 7.17]	60.3 [45.2; 80.6]	3.07 [2.72; 3.46]	2.10 [1.76; 2.50]
Model 2				
FDep				
Quintile 1	Ref.	Ref.	Ref.	Ref.
Quintile 2	0.96 [0.80; 1.15]	1.88 [1.43; 2.47]	0.93 [0.73; 1.17]	0.42 [0.29; 0.59]
Quintile 3	0.80 [0.65; 0.98]	0.59 [0.42; 0.84]	0.69 [0.55; 0.86]	0.19 [0.14; 0.27]
Quintile 4	0.42 [0.33; 0.52]	1.22 [0.88; 1.69]	0.73 [0.59; 0.91]	0.15 [0.11; 0.21]
Quintile 5	0.60 [0.50; 0.73]	0.11 [0.08; 0.15]	0.73 [0.57; 0.92]	0.20 [0.14; 0.29]
ΔNDVI exposure (lack of vegetation)				
Low	Ref.	Ref.	Ref.	Ref.
Medium	2.59 [2.46; 2.73]	5.83 [5.43; 6.26]	1.34 [1.27; 1.42]	1.54 [1.42; 1.68]
High	4.95 [4.67; 5.24]	27.6 [25.6; 29.9]	0.99 [0.93; 1.05]	1.56 [1.43; 1.70]
$\Delta\text{PM}_{2.5}$ exposure				
Low	Ref.	Ref.	Ref.	Ref.
Medium	0.58 [0.53; 0.64]	0.73 [0.64; 0.83]	4.67 [4.12; 5.30]	8.95 [7.42; 10.8]
High	1.01 [0.91; 1.12]	1.18 [1.03; 1.35]	7.84 [6.86; 8.96]	6.10 [5.16; 7.22]
ΔNO_2 exposure				
Low	Ref.	Ref.	Ref.	Ref.
Medium	1.03 [0.95; 1.12]	1.33 [1.20; 1.48]	0.78 [0.73; 0.82]	1.39 [1.27; 1.52]
High	0.59 [0.54; 0.64]	0.38 [0.34; 0.43]	0.89 [0.83; 0.95]	2.40 [2.16; 2.67]
ΔO_3 exposure				
Low	Ref.	Ref.	Ref.	Ref.
Medium	1.64 [1.49; 1.81]	2.78 [2.34; 3.30]	1.03 [0.87; 1.22]	0.56 [0.43; 0.72]
High	3.08 [2.78; 3.40]	25.0 [21.0; 29.8]	1.08 [0.92; 1.28]	1.79 [1.39; 2.31]

350 ^aOR (95% CI) estimated by non-ordinal polytomous logistic models.

351

352 DISCUSSION

353 Our findings showed that overexposure to heat was higher for the period 2015-2018 compared with the
354 other periods, which is consistent with the climatic trends observed in France (36, 37). The year 2003
355 showed a sharp increase in summer $\Delta\text{T}_{\text{mean}}$ and air pollutants and a decrease in summer ΔNDVI . This

356 year was marked by a severe heatwave in Europe and France, which led to 15,000 excess deaths in
357 France alone (38). These abnormally high temperatures explain the decrease in NDVI due to the drought,
358 the increase in O₃ concentrations (20), and more generally, the rise in all air pollutants. This increase in
359 air pollutants was probably due to the generation of O₃ (20), the lower absorption of pollutants by
360 drought-affected vegetation, and the soil mineral dust resuspension caused by the drought, limited
361 dispersion, and washing of particulate matter. Until 2018, we also observed a continuous and large
362 decrease in air pollutant concentrations for PM and NO₂ (two- to tenfold reduction on average depending
363 on the pollutant and urbanization level), which reflects the impact of successive action plans in various
364 sectors to improve air quality in France (39). However, most IRIS still exceeded the most recent WHO
365 air quality guidelines in 2018 (20% to 100% of IRIS depending on the pollutant and urbanization level).

366 On average, more than 4 million people lived in hotspots, i.e., areas cumulating adverse overexposure
367 to all environmental determinants. This study confirmed that between 2000-2018, urban IRIS were
368 generally more exposed to heat during summer and to air pollution throughout the year, while they had
369 less vegetation than rural IRIS. Differential exposure was greater in urban areas than in rural areas,
370 showing that environmental inequities were stronger in the urban environment. In urban areas, greater
371 deprivation was strongly associated with the risk of living in a hotspot or having more cumulative
372 exposure but only when using the EDI and not the FDep. In rural areas, the associations were more
373 consistent but inverted: greater deprivation measured by both the EDI and FDep was associated with a
374 lower risk of living in a hotspot. With the cumulative exposure indicator in rural areas, a U-shaped
375 relationship and a lower risk of cumulative exposure were observed with the EDI and FDep,
376 respectively.

377 In urban areas, our results support the findings of several studies that have identified associations
378 between heat, air pollution, or low vegetation/green space availability and social deprivation, with higher
379 exposure levels being linked to the most deprived populations (3-7, 40). However, some studies found
380 reverse associations, showing, for example, that less deprived populations have greater exposure or that
381 both the least and the most deprived populations have a greater exposure to air pollution (6, 40).

382 The differences observed between the two deprivation indices, which have already been discussed in
383 other studies (33, 34), can be explained by several reasons related to their construction methods. First,
384 the EDI was built to allow comparability between European countries (30), whereas the FDep was
385 created to characterize spatial socioeconomic heterogeneity in France (31). Second, these two indices
386 were estimated using different statistical methods. The EDI combines ten ecological weighted
387 socioeconomic and material variables based on census studies (30), whereas the FDep is based on four
388 ecological variables from principal component analysis (31). Finally, the components included in the
389 two indices also differ. For example, the EDI includes “the proportion of non-homeowners,” “the
390 proportion of households without a car,” and “the proportion of primary residences with more than one

391 person per room,” although these items do not reflect socioeconomic deprivation in the same way in
392 rural and urban areas (33, 34, 41). For example, urban areas often have well-developed public transport
393 systems, which limits the need to own a car. By contrast, rural areas often lack public transport, and thus
394 not owning a car can reflect social deprivation, as it limits mobility. Nevertheless, the variable
395 “proportion of households without a car” does not contribute the most to this index. Overcrowded
396 dwellings and homeownership may also have different associations with social deprivation in rural
397 compared with urban areas. The variables contributing the most are overcrowded households and single-
398 parent households (42). The apparent protective effect of social deprivation (as estimated by the EDI
399 and FDep) in rural areas can be explained by the specific spatial distribution of environmental exposures
400 and social deprivation. For example, low-density areas located far from attractive poles of activity tend
401 to be more vegetated and less affected by urban heat islands and air pollution, although their low housing
402 costs may attract residents with higher social deprivation scores. At the same time, IRIS closer to urban
403 poles or attractive areas (e.g., tourist zones) may be more exposed to deleterious environmental factors
404 but may also attract residents with a higher socioeconomic status.

405 In urban areas, highly socially deprived IRIS were less likely to be highly exposed to heat using the
406 EDI. IRIS overexposed to heat were also overexposed to a lack of vegetation in both rural and urban
407 areas. Surprisingly, in urban areas, high exposure to NO₂ or PM_{2.5} was negatively associated with
408 medium or high exposure to heat. Medium and high exposure to O₃ was associated with medium or high
409 exposure to heat.

410 Our methods have several limitations. First, we estimated the relative exposure of each IRIS population
411 based on the area-weighted average of temperatures, air pollution, and NDVI rather than the population-
412 weighted average. This may have under- or overestimated the exposure in some IRIS. Using the IRIS
413 as a spatial unit may also mischaracterize some levels of exposure, because rural IRIS have larger areas
414 and somewhat smaller populations compared with IRIS in towns and cities.

415 Second, the reference values for temperature were calculated over the period 2000-2018, including the
416 2003 heatwave, which was the most severe and deadliest heatwave episode in France’s history, as well
417 as other particularly warm years (2006, 2018). This could have increased the reference values and thus
418 lead to an underestimation of the relative exposure to temperature. Likewise, it might have
419 underestimated the number of hotspots for the 2000-2004 period.

420 Several limitations can be attributed to the use of the FDep and EDI. First, we used a constant value for
421 each index and IRIS over the entire study period, since annual values using 2021 geography references
422 were not available, and little change was found in the EDI values in 2009, 2013, and 2017 and the FDep
423 values between 2011 and 2017. Second, these indicators seem less adapted to rural areas, which might
424 introduce an approximation bias into their representativeness of rural and urban areas (32). Finally, the
425 EDI was not computed for large, sparsely populated IRIS with forests and leisure parks.

426 We assumed that population density was stable over the entire study period. Given the lack of data at
427 the IRIS level before 2014, we assumed that all IRIS in a given municipality changed population at the
428 same annual rate as the municipality. We also assumed that the population of each IRIS was constant
429 prior to 2006 due to the lack of harmonized census data for this period.

430 Finally, $\Delta PM_{2.5}$ was underestimated before 2008-2009 and ΔPM_{10} before 2007, because the semi-
431 volatile PM fraction was not yet measured. This underestimation represents about 30% of the annual
432 mean of PM_{10} (43, 44). No such evaluation was performed for $PM_{2.5}$. Consequently, the number of IRIS
433 overexposed to PM might have been slightly underestimated before 2009 in our study. Our exposure
434 indicators are proxies for population exposure and do not reflect the true daily exposure, which likely
435 varies between individuals in each IRIS. For example, a poor resident of an IRIS living in poorly
436 ventilated and insulated housing in a dense neighborhood and working in an outdoor job will be more
437 exposed to heat and air pollution than a wealthier resident of the same IRIS, even though both would be
438 assigned the same exposure level (40).

439 Our study has several strengths. Characterizing the socioeconomic and environmental burden of
440 populations at a fine scale and in a comparable manner highlights the environmental justice issues and
441 public health concerns of environmental exposures. To our knowledge, this is the first study to identify
442 hotspots of exposure to heat, air pollution, and lack of vegetation and their associations with social
443 deprivation. For instance, population-weighted summer temperatures and population-weighted NDVI at
444 the national level are currently monitored by the Lancet countdown as relevant indicators of climate
445 change impacts and adaptation policies, respectively (45). However, the Lancet countdown fails to
446 consider co-exposure, and the indicators are not always comparable across space. For instance, a given
447 temperature and a given NDVI have different impacts depending on the underlying climate and type of
448 vegetation.

449 We used exposure data at a fine spatiotemporal scale over a long period of time and across continental
450 France. These data were aggregated at the finest spatial administrative level available in France. We
451 used relative exposure indicators for NDVI and temperature to ensure comparability across areas and
452 climate types, while for air pollutants, we assessed exposure relative to the WHO guidelines that relate
453 to the underlying health risks. This approach is useful to study the effect of heat, air pollution, and lack
454 of vegetation on health outcomes.

455 This study provides the first overview of fine-scale exposure to heat stress and its co-exposures at a
456 national level. Hotspots, which represent the areas with the strongest environmental inequities, were
457 identified. This approach can support the inclusion of environmental inequities into adaptation strategies
458 to climate change.

459

460 **DATA AVAILABILITY STATEMENT**

461 The datasets generated during and analyzed during the current study are available from the
462 corresponding author on reasonable request.

463

464 **REFERENCES**

- 465 1. Ganzleben C, Kazmierczak A. Leaving no one behind – understanding environmental inequality
466 in Europe. *Environmental Health*. 2020;19(1):57.
- 467 2. EEA. Unequal exposure and unequal impacts: social vulnerability to air pollution, noise and
468 extreme temperatures in Europe. Copenhagen: EEA; 2018. Report No.: 22.
- 469 3. Hsu A, Sheriff G, Chakraborty T, Manya D. Disproportionate exposure to urban heat island
470 intensity across major US cities. *Nature Communications*. 2021;12(1):2721.
- 471 4. Venter ZS, Figari H, Krange O, Gundersen V. Environmental justice in a very green city: Spatial
472 inequality in exposure to urban nature, air pollution and heat in Oslo, Norway. *Science of The Total
473 Environment*. 2023;858:160193.
- 474 5. Schüle SA, Hilz LK, Dreger S, Bolte G. Social Inequalities in Environmental Resources of
475 Green and Blue Spaces: A Review of Evidence in the WHO European Region. *International Journal of
476 Environmental Research and Public Health* [Internet]. 2019; 16(7).
- 477 6. Padilla CM, Kihal-Talantikite W, Vieira VM, Rossello P, Nir GL, Zmirou-Navier D, et al. Air
478 quality and social deprivation in four French metropolitan areas—A localized spatio-temporal
479 environmental inequality analysis. *Environmental Research*. 2014;134:315-24.
- 480 7. Brunt H, Barnes J, Jones SJ, Longhurst JWS, Scally G, Hayes E. Air pollution, deprivation and
481 health: understanding relationships to add value to local air quality management policy and practice in
482 Wales, UK. *Journal of Public Health*. 2017;39(3):485-97.
- 483 8. Ebi KL, Capon A, Berry P, Broderick C, de Dear R, Havenith G, et al. Hot weather and heat
484 extremes: health risks. *Lancet*. 2021;398(10301):698-708.
- 485 9. EEA. Healthy environment, healthy lives: how the environment influences health and well-
486 being in Europe. Copenhagen; 2020. Report No.: 21.
- 487 10. Son J-Y, Liu JC, Bell ML. Temperature-related mortality: a systematic review and investigation
488 of effect modifiers. *Environmental Research Letters*. 2019;14(7):073004.
- 489 11. Analitis A, De' Donato F, Scortichini M, Lanki T, Basagana X, Ballester F, et al. Synergistic
490 Effects of Ambient Temperature and Air Pollution on Health in Europe: Results from the PHASE
491 Project. *International Journal of Environmental Research and Public Health* [Internet]. 2018; 15(9).
- 492 12. Pascal M, Gorla S, Wagner V, Sabastia M, Guillet A, Cordeau E, et al. Greening is a promising
493 but likely insufficient adaptation strategy to limit the health impacts of extreme heat. *Environment
494 International*. 2021;151:106441.
- 495 13. Schinasi LH, Benmarhnia T, De Roos AJ. Modification of the association between high ambient
496 temperature and health by urban microclimate indicators: A systematic review and meta-analysis.
497 *Environmental Research*. 2018;161:168-80.
- 498 14. Kumar P, Druckman A, Gallagher J, Gatersleben B, Allison S, Eisenman TS, et al. The nexus
499 between air pollution, green infrastructure and human health. *Environ Int*. 2019;133(Pt A):105181.

- 500 15. WHO. Urban green spaces and health. A review of evidence. Copenhagen: WHO Regional
501 Office for Europe; 2016.
- 502 16. Lalloué B, Monnez JM, Padilla C, Kihal W, Zmirou-Navier D, Deguen S. Data analysis
503 techniques: a tool for cumulative exposure assessment. *J Expo Sci Environ Epidemiol*. 2015;25(2):222-
504 30.
- 505 17. Jay O, Capon A, Berry P, Broderick C, de Dear R, Havenith G, et al. Reducing the health effects
506 of hot weather and heat extremes: from personal cooling strategies to green cities. *Lancet*.
507 2021;398(10301):709-24.
- 508 18. Markevych I, Schoierer J, Hartig T, Chudnovsky A, Hystad P, Dzhambov AM, et al. Exploring
509 pathways linking greenspace to health: Theoretical and methodological guidance. *Environ Res*.
510 2017;158:301-17.
- 511 19. Corso M, Pascal M. Agir pour le climat et la qualité de l'air pour la santé de tous. *La revue de*
512 *l'infirmière*. 2020;69(262):p. 24-6.
- 513 20. Monks PS, Archibald AT, Colette A, Cooper O, Coyle M, Derwent R, et al. Tropospheric ozone
514 and its precursors from the urban to the global scale from air quality to short-lived climate forcer. *Atmos*
515 *Chem Phys*. 2015;15(15):8889-973.
- 516 21. Insee. IRIS 2016 [Available from: <https://www.insee.fr/fr/metadonnees/definition/c1523>].
- 517 22. Insee. La grille communale de densité à 4 niveaux 2022 [Available from:
518 <https://www.insee.fr/fr/information/2114627>].
- 519 23. Insee. Recensement de la population 2022 [Available from:
520 <https://www.insee.fr/fr/information/2880845>].
- 521 24. Joly D, Brossard T, Cardot H, Cavailles J, Hilal M, Wavresky P. Les types de climats en France,
522 une construction spatiale. *Cybergeo : European Journal of Geography*. 2010.
- 523 25. Hough I, Just AC, Zhou B, Dorman M, Lepeule J, Kloog I. A multi-resolution air temperature
524 model for France from MODIS and Landsat thermal data. *Environ Res*. 2020;183:109244.
- 525 26. Robinson NP, Allred BW, Jones MO, Moreno Á, Kimball JS, Naugle DE, et al. A Dynamic
526 Landsat Derived Normalized Difference Vegetation Index (NDVI) Product for the Conterminous United
527 States. *Remote Sens*. 2017;9:863.
- 528 27. Hough I, Sarafian R, Shtein A, Zhou B, Lepeule J, Kloog I. Gaussian Markov random fields
529 improve ensemble predictions of daily 1 km PM_{2.5} and PM₁₀ across France. *Atmospheric*
530 *Environment*. 2021;264:118693.
- 531 28. Favez O, Cachier H, Sciare J, Le Moullec Y. Characterization and contribution to PM_{2.5} of
532 semi-volatile aerosols in Paris (France). *Atmospheric Environment*. 2007;41(36):7969-76.
- 533 29. Real E, Couvidat F, Ung A, Malherbe L, Raux B, Gressent A, et al. Historical reconstruction of
534 background air pollution over France for 2000–2015. *Earth Syst Sci Data*. 2022;14(5):2419-43.

- 535 30. Pernet C, Delpierre C, Dejardin O, Grosclaude P, Launay L, Guittet L, et al. Construction of an
536 adaptable European transnational ecological deprivation index: the French version. *J Epidemiol*
537 *Community Health*. 2012;66(11):982-9.
- 538 31. Rey G, Jouglu E, Fouillet A, Hémon D. Ecological association between a deprivation index and
539 mortality in France over the period 1997 – 2001: variations with spatial scale, degree of urbanicity, age,
540 gender and cause of death. *BMC Public Health*. 2009.
- 541 32. Gorza M, Eilstein D. Outils élaborés dans la cadre du programme « Inégalités sociales de santé
542 », 2013-2015. Saint-Maurice: Santé publique France; 2018.
- 543 33. Barry Y, Le Strat Y, Azria E, Gorza M, Pilkington H, Vandentorren S, et al. Ability of
544 municipality-level deprivation indices to capture social inequalities in perinatal health in France:
545 A nationwide study using preterm birth and small for gestational age to illustrate their relevance. *BMC*
546 *Public Health*. 2022;22(1):919.
- 547 34. Temam S, Varraso R, Pernet C, Sanchez M, Affret A, Jacquemin B, et al. Ability of ecological
548 deprivation indices to measure social inequalities in a French cohort. *BMC Public Health*.
549 2017;17(1):956.
- 550 35. WHO. WHO global air quality guidelines. Particulate matter (PM2.5 and PM10), ozone,
551 nitrogen dioxide, sulfur dioxide and carbon monoxide. . Geneva, Switzerland: World Health
552 Organization; 2021.
- 553 36. Sorel M, Soubeyroux J-M, Drouin A, Jourdain S, Kerdoncuff M, Cassaigne B, et al. Normales
554 climatiques 1991-2020., 119, 73-79, 2022. . *La Météorologie*. 2022;119:73-9.
- 555 37. Ribes A, Boé J, Qasmi S, Dubuisson B, Douville H, Terray L. An updated assessment of past
556 and future warming over France based on a regional observational constraint. *Earth Syst Dynam*.
557 2022;13(4):1397-415.
- 558 38. Fouillet A, Rey G, Laurent F, Pavillon G, Bellec S, Guihenneuc-Jouyaux C, et al. Excess
559 mortality related to the August 2003 heat wave in France. *Int Arch Occup Environ Health*.
560 2006;80(1):16-24.
- 561 39. comptes Cd. Les politiques de lutte contre la pollution de l'air. Cour des comptes; 2020.
- 562 40. Deguen S, Zmirou-Navier D. Social inequalities resulting from health risks related to ambient
563 air quality-A European review. *European Journal of Public Health*. 2010;20(1):27-35.
- 564 41. Gilthorpe MS, Wilson RC. Rural/urban differences in the association between deprivation and
565 healthcare utilisation. *Soc Sci Med*. 2003;57(11):2055-63.
- 566 42. Merville O, Launay L, Dejardin O, Rollet Q, Bryère J, Guillaume É, et al. Can an Ecological
567 Index of Deprivation Be Used at the Country Level? The Case of the French Version of the European
568 Deprivation Index (F-EDI). *Int J Environ Res Public Health*. 2022;19(4).
- 569 43. Malherbe L, Beauchamp M, Bourin A, Sauvage S. Analyse de tendances nationales en matière
570 de qualité de l'air. 2017.

571 44. Bessagnet B, Malherbe L, Aymoz G. Bilan de la première année de mesure des PM10 ajustées
572 en France et évaluation des outils de modélisation. 2008.

573 45. Countdown TL. Lancet Countdown: Tracking Progress on Health and Climate change
574 [Available from: [https://www.lancetcountdown.org/data-platform/adaptation-planning-and-resilience-](https://www.lancetcountdown.org/data-platform/adaptation-planning-and-resilience-for-health)
575 [for-health](https://www.lancetcountdown.org/data-platform/adaptation-planning-and-resilience-for-health)].

576

577

578 **ACKNOWLEDGEMENTS**

579 This work is part of a PhD thesis associated with the Doctoral Network in Public Health coordinated by
580 the Public Health School EHESP. The authors would like to thank INERIS (French Institute for
581 Industrial Environment and Risks) for commenting on the manuscript and making available in open data
582 the air pollutant concentration data from which the NO₂ and O₃ concentrations used in this study were
583 taken: [https://www.ineris.fr/fr/recherche-appui/risques-chroniques/mesure-prevision-qualite-
584 air/qualite-air-france-metropolitaine](https://www.ineris.fr/fr/recherche-appui/risques-chroniques/mesure-prevision-qualite-air/qualite-air-france-metropolitaine). The authors also acknowledge the French League against Cancer
585 (Ligue nationale contre le cancer).

586 The graphical abstract was designed using images from Flaticon.com.

587

588 **AUTHOR CONTRIBUTION STATEMENT**

589 LA, MP and JL designed and conceived this study with support from GF. LA conducted the analysis
590 and prepared the original draft of the manuscript with support from MP and JL. IH and ES contributed
591 to data curation. IH, ES, JL and IK acquired the data. LA, IH, ES, GF, GL, LL, MP and JL interpreted
592 the results. IH, ES, GF, IK, GL, LL, MP and JL reviewed the manuscript and provided substantial
593 feedback. All authors read and approved the final manuscript.

594

595 **FUNDING**

596 This work is part of a PhD thesis funded by Santé publique France (French Public Health Agency).

597

598 **COMPETING INTERESTS**

599 The authors declare that they have no known competing financial interests or personal relationships that
600 could have appeared to influence the work reported in this paper.

601